Chemical Physics 175 (1993) 13–21
North-Holland

Reaction dynamics of vibrationally excited H_2

Klaus Mikulecky and Karl-Heinz Gericke

Institut für Physikalische und Theoretische Chemie der Johann Wolfgang Goethe-Universität, Marie-Curie-strasse 11, D-60439 Frankfurt am Main 50, Germany

Received 26 February 1993

The quantum state resolved product state distribution of the reactions $O(^1D)+H_2(v=0,1)\rightarrow OH(^2\Pi, v, J, \Omega, \Lambda)+H$ and $C(^1D)+H_2(v=0,1)\rightarrow CH(^2\Pi, v, J, \Omega, \Lambda)+H$ were analysed by laser-induced fluorescence. For studying the influence of vibrational excitation on the reaction dynamics, H_2 was excited to its first vibrational state via stimulated Raman pumping. For both reactions $H_2(v=1)$ increases the reaction rate, but diminishes the Λ selectivity. Insertion of the atomic collision partner into the H_2 bond is the major reaction mechanism, but the probability for an abstraction process seems to increase when H_2 is vibrationally excited. The influence of translational energy on the reaction dynamics is observed for product states near the energetical limit. In the case of $O(^1D)+H_2$ a significant amount of collision energy is transferred into OH rotation, while the reaction of $C(^1D)+H_2$ transfers translational energy into vibrationally excited CH products.

1. Introduction

Compared to the reaction dynamics of species in their vibrational ground state our knowledge of the behaviour of vibrationally excited molecules is very limited up to now. Little is known about the influence of the center-of-mass kinetic energy of the reactants on the energy partitioning and fine-structure distribution of the products. In the past there have been several investigations on the influence of vibrational energy on chemical reactions, but in general these were kinetic measurements. Experiments on a state-to-state level are rare [1–5]. There are a number of review articles on vibrational activation in bimolecular reactions [6–11].

Preparation of a reactant in a single rotational-vibrational state is possible by laser excitation. Molecules that show an IR absorption, such as HCl and HF, may be excited by tunable IR radiation or by special single frequency lasers, for example HF laser. Molecules without a permanent dipole moment can be excited by stimulated Raman pumping (SRP) [12,13]. Beside stimulated emission pumping, there is, in fact, another technique to achieve selective rotational-vibrational excitation, the "stimulated Raman scattering involving adiabatic passage" method (STIRAP), which has been applied successfully for the excitation of Na_2 [14]. However, this technique is more complicated to handle because it requires high power cw lasers with narrow bandwidths. Other methods, like thermal excitation or Franck–Condon pumping (FCP), do not reach the high degree of selectivity required for state-to-state measurements.

Molecular hydrogen is a convenient reactant for experiments on vibrational excitation, as far as the magnitude of the prospective effects is concerned. The first vibrationally excited state of H_2 contains an energy of 4155 cm^{-1} above the ground state, which has to be partitioned among the different degrees of freedom of the reaction products. This is a considerable amount compared to the enthalpies ΔH_{298} of the chemical reactions which we investigated:

$$O(^1D)+H_2(v)\rightarrow OH(X\,^2\Pi, v'', J'')+H\,,$$
$$\Delta H_{298}=-15980\ cm^{-1}\ \text{with}\ H_2(v=0)\,,$$
$$\Delta H_{298}=-20130\ cm^{-1}\ \text{with}\ H_2(v=1)\,, \qquad (1)$$

and

$$C(^1D)+H_2(v)\rightarrow CH(X\,^2\Pi, v'', J'')+H\,,$$
$$\Delta H_{298}=-2040\ cm^{-1}\ \text{with}\ H_2(v=0)\,,$$
$$\Delta H_{298}=-6190\ cm^{-1}\ \text{with}\ H_2(v=1)\,. \qquad (2)$$

At $T=298$ K both reactions proceed with comparable gas-kinetic rate constants, about 1.1×10^{-10} cm^3 $molec^{-1}$ s^{-1} [15–18] for (1) and between 4.1×10^{-11} [19] and 2.6×10^{-10} cm^3 $molec^{-1}$ [20] for (2).

These reactions may serve as model systems for the interactions of electronically excited atoms A with diatomics BC where there is a stable molecule ABC as transition state. The system does not surmount a barrier, but proceeds through an energy valley:

$$A^* + BC(v) \rightarrow (ABC)^* \rightarrow AB(v,J) + C\,.$$

Here, the lowest singlet states of H_2O and CH_2 (both $^1A_1$) are the transition states. They are highly vibrationally excited and decay to the products rapidly. Of particular interest to us is the influence of the BC vibrational excitation on the reaction mechanism and energy disposal. Some information on the influence of translational energy on the reaction dynamics can be gained by observation of product states near the energy limit. It is the common opinion that both reactions proceed by insertion of the atom into the H_2 bond. The other possible mechanism, the abstraction of an H atom by $O(^1D)/C(^1D)$, can be excluded by experimental evidence and theoretical calculations, as will be pointed out in more detail in the discussion. We measured the rotational–vibrational population distribution of OH from reaction (1) in $v''=3$ and 4 because $P(v''=4)/P(v''=3)$ was unknown. Furthermore, the rotational product state distribution of these vibrational states can be observed up to the energy limit of the reaction where the largest influence of translational and vibrational reactant excitation is expected. The same arguments apply to the $v''=1$ state of CH from reaction (2).

There are a considerable number of papers on the dynamics of reaction (1), experimental [21–37] as well as theoretical work [38–52]. This reaction has attracted much more experimental and theoretical interest than the closely related reaction of atomic carbon. A reason for the predominant role of reaction (1) might be that of experimental convenience. No VUV radiation is required for the production of $O(^1D)$, as in the case of $C(^1D)$. Further, all the products from the ozone photolysis are volatile, whereas the carbon suboxide photolysis yields large amounts of solid carbon deposited on the walls and windows of the vacuum chamber. The VUV problem can be solved by two-photon dissociation of C_3O_2, as was described previously [53].

Our experimental work [54] related to the reaction of $H_2(v=0)$ was preceded by two research groups [55–57]. To our knowledge, there had been just one trajectory calculation performed [58]. Additionally, there are calculations of the $CH_2(\tilde{a}\,^1A_1)$ potential energy surface. $CH_2(\tilde{a}\,^1A_1)$ is an intermediate in reaction (2), because $C(^1D)$ is supposed to insert into the H_2 bond.

Reaction (2) is clearly favourable from the viewpoint of the possible effect of reactant vibrational excitation in the reaction dynamics. The amount of energy transferred into the system by exciting H_2 from $v=0$ to $v=1$ is more than twice the reaction enthalpy. The respective number for the $O(^1D)$ reaction is 26%.

2. Experimental

This section gives only an outline of the experimental procedures. Details of the experimental apparatus are given in previous publications [37,54]. Electronically excited oxygen and carbon atoms were produced in a pulsed laser photolysis of ozone and carbon suboxide, respectively. The photolysis wavelengths were 266 nm for O_3 and 157 nm for C_3O_2. The production of $C(^1D)$ causes considerably greater problems than in the case of $O(^1D)$. First, the VUV radiation of a fluorine laser (EMG 201 MSC, Lambda Physik) has to be conducted through a nitrogen-flushed pipe to avoid absorption in air. Second, the photodissociation of C_3O_2 yields not only volatile products as is the case in the O_3 photolysis. There is always a considerable amount of solid carbon deposited on the windows of the vacuum chamber and the lenses of the photomultiplier optics, resulting in regularly extensive cleaning of all optical components. Ozone was prepared in a silent discharge in O_2, carbon suboxide by the standard procedure of dehydrating malonic acid with subsequent distillation [59].

The products were probed by LIF with an excimer pumped dye laser (FL 2002 E, Lambda Physik) at time delays of 200 ns for reaction (1) and 360 ns for reaction (2). We excited the $(A\,^2\Sigma, v'=0,1) \leftarrow (X\,^2\Pi, v''=3,4)$ transitions of OH at wavelengths around 450 nm. The direct $\Delta v=0$ transitions starting from $v''=3$ or 4 are inaccessible by LIF because of strong predissociation of the Σ state [60–63]. CH was probed by the $(B\,^2\Sigma^-, v'=0, 1) \leftarrow (X\,^2\Pi, v''=0, 1)$ transitions at 390–400 nm [64–67].

The experiments with vibrationally excited H_2 were performed by focusing the frequency doubled output of an Nd:YAG laser (Spectron SL2Q) through an H_2 pressure Raman shifter into the vacuum chamber. The Stokes and anti-Stokes radiation of the Raman shifter excite H_2 from $v=0$ to $v=1$. An estimated portion of about 20% of the H_2 can be excited this way [1]. When investigating the carbon atom reaction we used a trigger-suspending device to perform very precise differential measurements of the $H_2(v=1)$ influence. This device triggered the Q-switch of the Nd:YAG laser used to excite H_2 on every second pulse only. So we obtained two data sets, one with $H_2(v=1)$ and the other with $H_2(v=0)$, within a single scan.

3. Results

3.1. Oxygen atom reaction

Normalizing the measured line intensities with respect to the transition probabilities for $(A\,^2\Sigma; v'=0, 1; J') \leftarrow (X\,^2\Pi; v''=3, 4; J'')$ yields the respective populations of the OH rotational states. The rotational population distribution of $OH(X\,^2\Pi; v''=3$ and 4) is shown in fig. 1. Additionally, the rotational prior distributions for the reactions of $O(^1D)$ with $H_2(v=0)$ and $H_2(v=1)$ are shown. The data of the measured rotational distribution were obtained by adding the populations of the Λ substates belonging to every rotational level. The measurements with and without $H_2(v=1)$ show essentially the same behaviour. There is a strongly inverted rotational distribution for $OH(v''=3)$, being less pronounced for $OH(v''=4)$. The vertical line in fig. 1 indicates the mean available energy E_{av}. E_{av} equals 15980 cm^{-1} for the reaction with $H_2(v=0)$ and 20130 cm^{-1} for $H_2(v=1)$. An interesting feature in the rotational state distribution is the population of rotational-vibrational states above E_{av}. This is essentially due to the Maxwell–Boltzmann velocity distribution of the hydrogen molecules. This will be considered in more detail in the discussion.

Summing up the populations of all rotational states

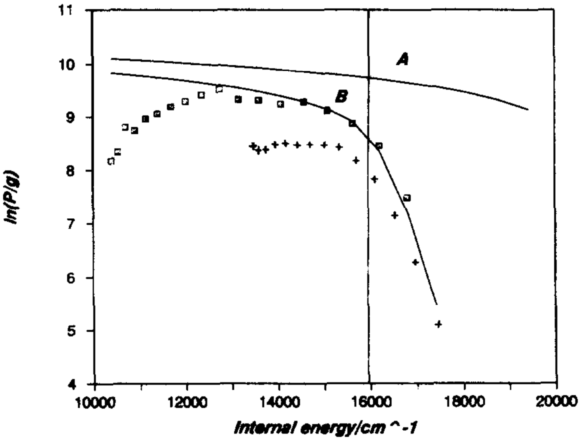

Fig. 1. Boltzmann plot of the rotational distribution of OH from reaction (1). Squares: $OH(v''=3)$, crosses: $OH(v''=4)$. The solid lines represent the result of prior calculations for $OH(v''=3)$ from the reaction with $H_2(v=1)$ (A) and $H_2(v=0)$ (B). The vertical line near 16000 cm^{-1} shows the exothermicity of the reaction. P: rotational state population, g: rotational state degeneracy.

yields the total population of the vibrational state. The vibrational population numbers are a quite crucial feature because they are very sensitive to the Franck–Condon factors of the related transitions. The transition probabilities are reported quite differently in the literature, as was mentioned in previous papers [68,69]. We obtained a population ratio $P(v''=4)/P(v''=3)=0.28$ for the reaction of $H_2(v=0)$ and $P(v''=4)/P(v''=3)=0.33$ for the reaction of $H_2(v=1)$. This difference in the populations of about 15% has to be related to the excitation efficiency for the generation of $H_2(v=1)$ of about 20%. So we calculate an increase in the vibrational excitation of about 70% when there is only $H_2(v=1)$ as a reaction partner for $O(^1D)$. Despite the fact that the real concentration of $H_2(v=1)$ is not exactly known it is clear that vibrationally excited H_2 influences the vibrational distribution considerably. It should be mentioned that Franck–Condon factors are unimportant for a comparison of $H_2(v=0)$ and $H_2(v=1)$.

There are two types of electronic fine structure distribution to be considered for the OH molecule. The first one is the spin–orbit splitting. No deviations from the statistically expected population of the two spin systems $^2\Pi_{1/2}$ and $^2\Pi_{3/2}$ are observed. The second one is the Λ doubling emerging from the interaction between orbital angular momentum and nuclear rotation. The different behaviour of the Λ sublevels is well characterized by the difference of the individual population $P(\Pi(\mathrm{A}))$ probed by the Q and P or R branches:

$$f_\Lambda = \frac{P(\Pi(\mathrm{A}'')) - P(\Pi(\mathrm{A}'))}{P(\Pi(\mathrm{A}'')) + P(\Pi(\mathrm{A}'))} .$$

A negative value of f_Λ indicates a preferred generation of products in the $\Pi(\mathrm{A}')$ state which is symmetric with respect to reflection of the wavefunction on the plane of rotation. In the case of OH, P and R lines probe the symmetric Λ component and Q lines probe the antisymmetric $\Pi(\mathrm{A}'')$ sublevel. In the case of CH products, probing of the Λ sublevels is reversed: Q lines analyse the $\Pi(\mathrm{A}')$ component and P, R lines probe the $\Pi(\mathrm{A}'')$ sublevel. The solid lines in fig. 2 indicate the observed ratio f_Λ for the reaction of $O(^1D)$ and $C(^1D)$ with $H_2(v=0)$ and the symbols represent the reactions of vibrationally excited $H_2(v=1)$. The Λ sublevels showed to be populated selectively, most of the OH generated in reaction (1) was found in the $\Pi(\mathrm{A}')$ states which are symmetric with respect to the plane of reaction.

Obviously the Λ selectivity is much less pronounced for the $C(^1D)+H_2$ reaction. At high product rotations the Λ selectivity decreases for both reactions when vibrationally excited H_2 is used as reaction partner.

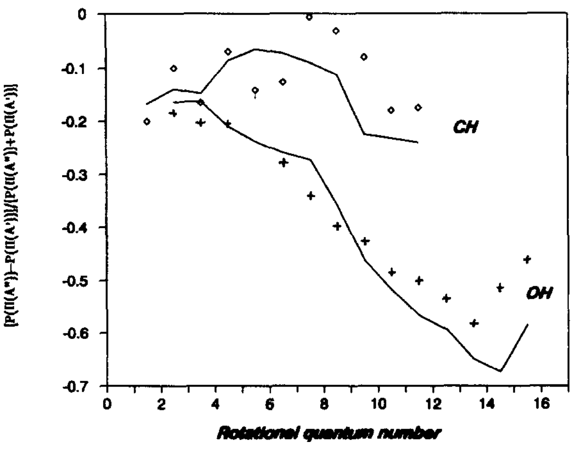

Fig. 2. Plot of the Λ-state distribution for the reaction products OH and CH. The solid lines represent the distributions for the reactions with $H_2(v=0)$, the symbols show the distributions for the reactions with $H_2(v=1)$.

3.2. Carbon atom reaction

The rotational state distribution of $CH(v''=0)$ from reaction (2) can approximately be described by a Boltzmann distribution except for the highest observed states, $N''=12$ to 14. We found temperature parameters of 1930 ± 190 K for the $\Pi(\mathrm{A}')$ states and 1230 ± 100 K for $\Pi(\mathrm{A}'')$ states. Only a very small quantity of $CH(v''=1)$ is generated in this reaction: $P(v''=1)/P(v''=0)=4.1\times10^{-4}$. The rotational population of $CH(v''=1)$ is also described by a Boltzmann distribution. We found a temperature parameter of 340 K. As was mentioned in the experimental section, very precise measurements on the influence of $H_2(v=1)$ on this reaction were carried out by using a trigger suspender for the H_2 exciting YAG laser. So we observed that the presence of $H_2(v=1)$ in reaction (2) increased the amount of CH by 1% for the lower rotational states, increasing to 3% for $N''=12$. There was no observable effect on the CH population ratio $P(v''=1)/P(v''=0)$. The rotational state distribution of CH is shown in fig. 3.

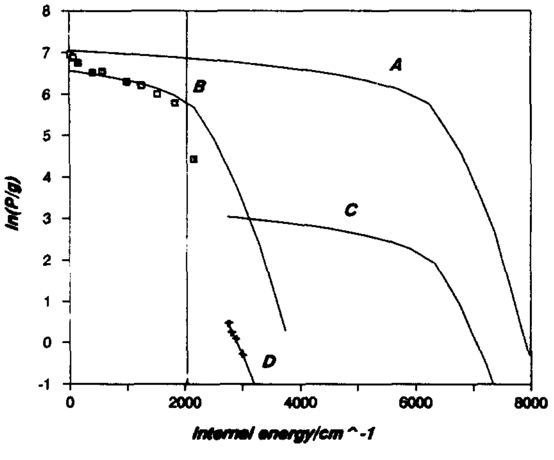

Fig. 3. Boltzmann plot of the rotational distribution of CH from reaction (2). Squares: $CH(v''=0)$, crosses: $CH(v''=1)$. The solid lines represent the following prior distributions. (A) $CH(v''=0)$ from $C(^1D)+H_2(v=1)$; (B) $CH(v''=0)$ from $C(^1D)+H_2(v=0)$; (C) $CH(v''=1)$ from $C(^1D)+H_2(v=1)$; (D) $CH(v''=1)$ from $C(^1D)+H_2(v=0)$. The exothermicity of the reaction is indicated by the vertical line near 2000 cm^{-1}. P: rotational state population, g: rotational state degeneracy.

For CH, there are the same types of electronic fine structure as for OH. The CH generated by reaction (2) does not show any selectivity concerning the distribution over the spin–orbit states f_1 and f_2. There is a very weak preponderance of the f_1 levels, but this is due to the lower energy of the f_1 relative to the f_2 system.

The population of the Λ sublevels is significantly less pronounced as in the case of $O(^1D)+H_2$. Only at very high rotations the CH product molecule is preferentially generated with (pπ)-orbital aligned in the plane of reaction, i.e. in the symmetric $\Pi(A')$ state. There is an influence of $H_2(v=1)$ on the population distribution of the Λ states. The already low selectivity decreases even more when there is vibrationally excited H_2 present in the reaction.

4. Discussion

The reactions that have to be discussed here are very closely related to each other. There are similarities in the electronic structure of the reactants (^1D) and products ($^2\Pi$) as well as in the properties of the collision complex (a deep well); nevertheless, we obtained quite different results as far as the internal energy distribution is concerned. The oxygen atom reaction generates a strong inversion of the OH rotational state distribution. Commonly this is regarded as a sign of nonstatistical influences. However, calculations indicate that the conservation of angular momentum of the H–O–H transition state requires a large rotational excitation of the OH product [47]. Even a statistical distribution of the available energy to the degrees of freedom does not affect this dynamical phenomenon. The vibrational energy distribution between $OH(v''=3)$ and $OH(v''=4)$ can be better reproduced by a prior distribution than the rotational energy (fig. 1). The measured population ratio $P_{exp}(v''=4)/P_{exp}(v''=3)=0.28$ is slightly below the result of a prior calculation which yields 0.34 for the population ratio, when only $H_2(v=0)$ is considered. Thus the statistical model reproduces approximately the behaviour of the reaction.

For a mixture of 20% $H_2(v=1)$ and 80% $H_2(v=0)$ the calculated ratio increases from 0.34 to 0.60. Experimentally the ratio $P(v=4)/P(v=3)\approx0.28$ increases to 0.33 when vibrationally excited H_2 is used. Obviously, there is only poor agreement between the statistical expectation and the measured value. This behaviour is even more pronounced for the rotational distribution. The prior distribution $P^0(v''=3, J'')$ for $H_2(v=0)$ (curve B in fig. 1) describes qualitatively the general trend of the observed OH rotational distribution (squares in fig. 1). According to a prior calculation reactions of vibrationally excited H_2 should result in a significant increase in product rotation (curve A in fig. 1). However, the opposite is observed in the experiment.

The $CH(v, J)$ product state distribution in the $C(^1D)+H_2(v=0)$ reaction is also reproduced by a prior calculation which can be recognized in fig. 3. However, a prior distribution of the reaction of $C(^1D)$ with $H_2(v=1)$ is completely inadequate to describe the population of CH product states (curves A and C in fig. 3).

The question whether there is an insertion of abstraction mechanism leading to the reaction products has been discussed extensively in the past. We assume an insertion mechanism for the reaction of $H_2(v=0)$ and an increasing probability of abstraction when the hydrogen molecule is vibrationally excited.

The reaction of vibrationally excited hydrogen leads to a higher vibrational excitation of OH; the population of $OH(v''=4)$ increases by 70% with respect to $OH(v''=3)$ if there were only $H_2(v=1)$ as reaction partner. Additionally, we observe a slight decrease in the OH rotational excitation for the reaction with $H_2(v=1)$. The most decisive argument for an insertion reaction mechanism is the product distribution of the Λ substates. Conservation of symmetry relative to the reaction plane requires the overall electronic state symmetry properties of the reactants to be maintained in the transition state and in the products. Hence, the symmetric reactants $O(^1D)$ and $H_2(^1\Sigma_g^+)$ yield a symmetric collision complex, $H_2O(^1A_1)$, that decays to symmetric products, $OH(\Pi(A'))$ and $H(^2S)$. This is represented by the correlation diagram in fig. 4. The only energetically accessible way from $O(^1D)+H_2$ to $OH(^2\Pi)+H$ leads through the $H_2O(\tilde{X}\,^1A_1)$ valley. The first excited singlet state of water, $H_2O(\tilde{A}\,^1B_1)$, has an energy of $\approx2400\ cm^{-1}$ above the reactant level [46]. It is not accessible by taking translational energy into account, but it may be accessible when there is vibra-

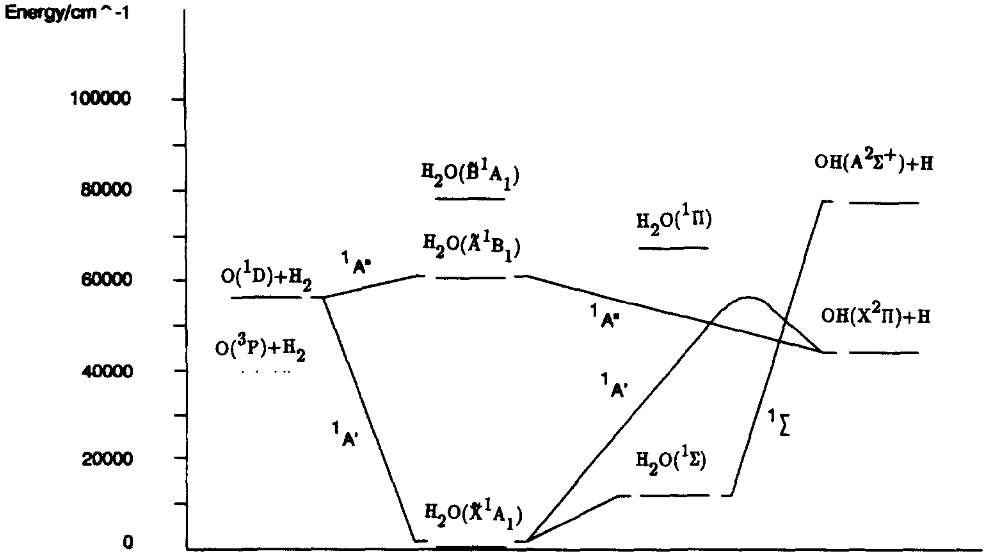

Fig. 4. Correlation diagram for reaction (1).

tionally excited H_2 present in the reaction. However, the path via the $\tilde{A}\,{}^1B_1$ state requires a different reaction symmetry.

Our observations are in qualitative agreement with theoretical calculations on this subject. Schinke and Lester [40] and Berg et al. [70] performed quasi-classical trajectory calculations for $H_2(v=1)$ in the former and for translationally, rotationally and vibrationally excited H_2 in the latter case. Schinke et al. found the population ratio $P(v''=4)/P(v''=3)=0.63$ for $H_2(v=0)$ to be inverted to 1.35 for $H_2(v=1)$. Berg et al. calculated a ratio of 0.34 for $H_2(v=0)$ and a value between 0.9 and 1 for $H_2(v=4)$.

A high vibrational excitation of the OH product is expected for an abstraction mechanism but not for an insertion process. A statistical distribution is less likely for a fast abstraction mechanism than for a long lived complex which is expected for an insertion mechanism via the $H_2O(^1A_1)$ surface. Especially the Λ selectivity has to vanish for a pure abstraction reaction because of symmetry reasons. Hence, there are several indications that the reaction dynamics change when vibrationally excited H_2 is used as reactant. "Head-on" collisions (O–HH) may become more favoured and contribute additionally to the OH product distribution.

This assumption is supported by the trajectory study of Berg et al. [69] where the $H_2(v)$ and $O(^1D)$ surface is found to be attractive for all reaction geometries. This attractive part of the potential extends even further for the collinear than for the perpendicular configuration. When $H_2(v=0)$ and $O(^1D)$ approach each other, the system reorientates towards a perpendicular configuration because the potential for this C_{2v} geometry is attractive, in contrast to a head-on collision where a potential barrier has to be passed [51]. H_2 reorientates more than one order of magnitude faster than it takes the reactants to pass each other.

In the course of the reaction $C(^1D)+H_2(v=0)$ the deep well of the $^1A_1$ surface is also involved and a similar reaction mechanism as for $O(^1D)+H_2$ is expected. On a first glance the experimental findings seem to contradict this assumption. The distribution of the energy with respect to the internal degrees of freedom results in an extremely weak vibrational excitation of $CH(^2\Pi)$ and a thermal rotational state distribution in $CH(v''=0)$ and $CH(v''=1)$. The vibrational energy content of CH is extremely small (1.1 cm^{-1}) and remains unaltered when using $H_2(v=1)$ for the reaction. The observed rotational energy increased from 707 to 813 cm^{-1} on exciting H_2. Pure $H_2(v=1)$ as reaction partner for $C(^1D)$ will result in a rotational energy content of 1240 cm^{-1}. The largest fraction of the product energy is found as translational energy of the CH–H system. $f_{trans}=E_{trans}/E_{av}$ is 0.74 for the reaction with $H_2(v=0)$ and 0.82 for the reaction with H_2 being exclusively in the first vibrationally excited state.

The differences between reactions (1) and (2) in terms of energy distribution can be explained by the different total available energy E_{av} which is 15980 cm^{-1} for the $O(^1D)$ and 2040 cm^{-1} for the $C(^1D)$ reaction with $H_2(v=0)$. From pure energy reasons no highly excited CH is possible.

Nevertheless, there is a considerable difference in the alignment of the $OH(^2\Pi)$ and $CH(^2\Pi)$ product molecules. We found a value of $f_A=-0.7$ for the high-J limit of OH from reaction (1), but reaction (2) produces CH with a maximum alignment of about $f_A=-0.25$. The less pronounced specificity in the production of $CH(\Pi(A'))$ does not necessarily imply a reaction mechanism proceeding via a linear collision geometry. Although a statistical population distribution between the $\Pi(A')$ and $\Pi(A'')$ states is expected in this case, the abstraction reaction will not be the major reaction path. This is because the linear collision geometry exhibits a late barrier in contrast to the C_{2v} surface which exhibits no barrier but a deep well at the $CH_2(\tilde{a}\,^1A_1)$ equilibrium configuration (fig. 5) [58,71]. The calculated height of the barrier (at least 40.5 kJ mol^{-1}) is well above the available energy E_{av} for $H_2(v=0)$ ($E_{av}=31.9$ kJ mol^{-1}). As a

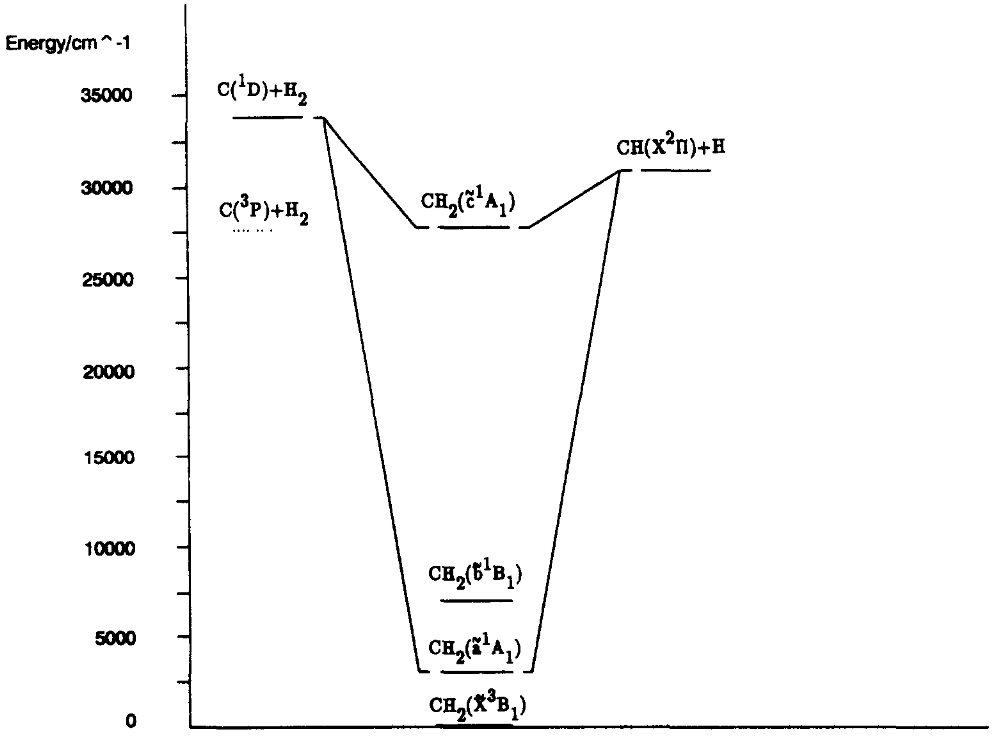

Fig. 5. Correlation diagram for reaction (2).

consequence, calculations of Whitlock et al. [58] indicate that 99% of all trajectories proceed via the insertion path.

Vibrationally excited H_2 supplies more than sufficient energy to pass the barrier. Furthermore, vibrational motion of the reactant accelerates reactions which involve a late barrier. An increase in the reaction rate is observed in the $H_2(v=1)$ experiments. Moreover, a decrease in the Λ selectivity is observed (similar to $O(^1D)+H_2$) when $H_2(v=1)$ is used. In total, it seems to be very likely that both the reaction $C(^1D)+H_2$ and the reaction $O(^1D)+H_2$ change the reaction geometry when vibrationally excited H_2 is the collision partner of the reactant molecule and an abstraction process becomes more important. The overall low Λ specificity in the $C(^1D)+H_2$ reaction is probably caused by interaction of the other low lying electronic states of CH_2 [53]. Fig. 5 shows a correlation diagram for the $C+H_2$ system. Especially, reactions via the stable $CH_2(\tilde{b}\,^1B_1)$ intermediate will diminish the preferred production of $CH(\Pi(A'))$.

Acknowledgement

This project was supported by the Deutsche Forschungsgemeinschaft (DFG) and the German Fonds der Chemischen Industrie. We thank Professor F.J. Comes for material support and helpful discussions.

References

[1] D.A.V. Kliner and R.N. Zare, J. Chem. Phys. 92 (1990) 2107.

[2] J.G. Pruett and R.N. Zare, J. Chem. Phys. 64 (1976) 1774.

[3] Z. Karny, R.C. Estler and R.N. Zare, J. Chem. Phys. 69 (1978) 5199.

[4] Z. Karny and R.N. Zare, J. Chem. Phys. 68 (1978) 3360.

[5] R. Zhang, D.J. Rakestraw, K.G. McKendrick and R.N. Zare, J. Chem. Phys. 89 (1988) 6283.

[6] M.J. Berry, Ann. Rev. Phys. Chem. 26 (1975) 259.

[7] M. Kneba and J. Wolfrum, Ann. Rev. Phys. Chem. 31 (1980) 47.

[8] J. Wolfrum, J. Phys. Chem. 90 (1986) 375.

[9] J. Wolfrum, Faraday Discussions Chem. Soc. 84 (1987) 191.

[10] I.W.M. Smith, in: Bimolecular collisions, eds. M.N.R. Ashfold and J.E. Baggott (The Royal Society of Chemistry, London, 1989).

[11] H.G. Rubahn and K. Bergmann, Ann. Rev. Phys. Chem. 41 (1990) 735.

[12] W. Meier, G. Ahlers and H. Zacharias, J. Chem. Phys. 85 (1986) 2599.

[13] Y. Zhu, Y. Huang, S. Arepalli and R.J. Gordon, J. Appl. Phys. 67 (1990) 604.

[14] P. Dittmann, F.P. Pesl, J. Martin, G.W. Coulston, G.Z. He and K. Bergmann, J. Chem. Phys. 97 (1992) 9472.

[15] J.A. Davidson, C.M. Sadowski, H.I. Schitt, G.E. Steit, C.J. Howard, D.A. Jennings and A.L. Schmeltekopf, J. Chem. Phys. 64 (1976) 57.

[16] R.F. Haidner and D. Husain, Intern. J. Chem. Kinetics 5 (1973) 819.

[17] L.J. Stief, W.A. Payne and R.B. Klemm, J. Chem. Phys. 62 (1975) 4000.

[18] R.A. Young, G. Black and T.G. Slanger, J. Chem. Phys. 49 (1986) 475.

[19] W. Braun, A.M. Bass, D.D. Davis and J.D. Simmons, Proc. Roy. Soc. A 312 (1969) 417.

[20] D. Husain and L.J. Kirsch, Chem. Phys. Letters 9 (1971) 412.

[21] G.D. Downey, D.W. Robinson and J.H. Smith, J. Chem. Phys. 66 (1977) 1685.

[22] G.K. Smith, J.E. Butler and M.C. Lin, Chem. Phys. Letters 65 (1979) 115.

[23] G.K. Smith and J.E. Butler, J. Chem. Phys. 73 (1980) 2243.

[24] A.C. Luntz, R. Schinke, W.A. Lester and H.H. Günthard, J. Chem. Phys. 70 (1979) 5908.

[25] R.J. Buss, P. Casavecchia, T. Hirooka, S.J. Sibener and Y.T. Lee, Chem. Phys. Letters 82 (1981) 386.

[26] J.E. Butler, R.G. MacDonald, D.J. Donaldson and J.J. Sloan, Chem. Phys. Letters 95 (1983) 183.

[27] K. Tsukiyama, B. Katz and R. Bersohn, J. Chem. Phys. 83 (1985) 2889.

[28] G.M. Jursich and J.R. Wiesenfeld, Chem. Phys. Letters 119 (1985) 511.

[29] J.E. Butler, G.M. Jursich, I.A. Watson and J.R. Wiesenfeld, J. Chem. Phys. 84 (1986) 5365.

[30] Y. Huang, Y. Gu, G. Lin, X. Yang and Y. Tao, Chem. Phys. Letters 127 (1986) 432.

[31] P.M. Aker and J.J. Sloan, J. Chem. Phys. 85 (1986) 142.

[32] C.B. Cleveland, G.M. Jursich, M. Trolier and J.R. Wiesenfeld, J. Chem. Phys. 86 (1987) 3253.

[33] J.J. Sloan, J. Phys. Chem. 92 (1988) 18.

[34] T.J. Sears, G.E. Hall and J.J.F. McAndrew, J. Chem. Phys. 91 (1989) 5201.

[35] A. Lebéhot, S. Drawin, Fa. Aguillon, R. Campargue and X. Chapuisat, J. Chem. Phys. 92 (1990) 7340.

[36] J. Shao, L. Yuan, H. Yang, Y. Gu, K. Li, K. Wang and Y. Tao, presented on the Informal Conference on Photochemistry, Atlanta, 1992, Conference Rep. N4.

[37] K. Mikulecky and K.-H. Gericke, J. Chem. Phys. 96 (1992) 7490.

[38] R.D. Levine, B.R. Johnson and R.B. Bernstein, Chem. Phys. Letters 19 (1973) 1.

[39] R.E. Howard, A.D. McLean and W.A. Lester, J. Chem. Phys. 71 (1979) 2412.

[40] R. Schinke and W.A. Lester, J. Chem. Phys. 72 (1980) 3754.
[41] J.N. Murrell, S. Carter, I.M. Mills and M.F. Guest, Mol. Phys. 42 (1981) 605.
[42] P.A. Whitlock, J.T. Muckerman and E.R. Fisher, J. Chem. Phys. 76 (1982) 4468.
[43] S.W. Ransome and J.S. Wright, J. Chem. Phys. 77 (1982) 6346.
[44] L.J. Dunne and J.N. Murrell, Mol. Phys. 50 (1983) 635.
[45] J.N. Murrell and S. Carter, J. Phys. Chem. 88 (1984) 4887.
[46] G. Durand and X. Chapuisat, Chem. Phys. 96 (1985) 381.
[47] K. Rynefors, P.A. Elofson and L. Holmlund, Chem. Phys. 100 (1985) 53.
[48] M.S. Fitzcharles and G.C. Schatz, J. Phys. Chem. 90 (1986) 3634.
[49] J.K. Badenhoop, H. Koizumi and G.C. Schatz, J. Chem. Phys. 91 (1989) 142.
[50] E. Goldfield and J.R. Wiesenfeld, J. Chem. Phys. 93 (1990) 1030.
[51] P.J. Kuntz, B.I. Niefer and J.J. Sloan, Chem. Phys. 151 (1991) 77.
[52] P.M. Aker, J.J. Sloan and J.S. Wright, Chem. Phys. 110 (1986) 275.
[53] D.C. Scott, J. de Juan, D.C. Robie, D. Schwartz-Lavi and H. Reisler, J. Phys. Chem. 96 (1992) 2509.
[54] K. Mikulecky and K.-H. Gericke, J. Chem. Phys. 98 (1993) 1244.
[55] G.M. Jursich and J.R. Weisenfeld, Chem. Phys. Letters 110 (1984) 14.
[56] G.M. Jursich and J.R. Weisenfeld, J. Chem. Phys. 83 (1985) 910.
[57] W.H. Fisher, T. Carrington and C.M. Sadowski, Chem. Phys. 97 (1985) 433.
[58] P.A. Whitlock, J.T. Muckerman and P.M. Kroger, in: Potential energy surfaces and dynamics calculations, ed. D.G. Truhlar (Plenum Press, New York, 1981).
[59] O. Diels and G. Meyerheim, Ber. Dt. Chem. Ges. 40 (1907) 355.
[60] J. Brzozowski, P. Erman and M. Lyyra, Phys. Scr. 17 (1978) 507.
[61] J.A. Coxon, Can. J. Phys. 58 (1980) 933.
[62] G.H. Dieke and H.M. Crosswhite, J. Quant. Spectry. Radiative Transfer 2 (1962) 97.
[63] W.L. Dimpfl and J.K. Kinsey, J. Quant. Spectry. Radiative Transfer 21 (1979) 233.
[64] G. Herzberg and J.W.C. Johns, Astrophys. J. 158 (1969) 399.
[65] P.F. Bernath, C.R. Brazier, T. Olsen, R. Hailey, W.T.M.L. Fernando, C. Woods and J.L. Hardwick, J. Mol. Spectry. 147 (1991) 16.
[66] L. Gerö, Z. Physik 118 (1941) 27.
[67] S.V. Filseth, H. Zacharias, J. Danon, R. Wallenstein and K.H. Welge, Chem. Phys. Letters 58 (1978) 140.
[68] K. Mikulecky, K.-H. Gericke and F.J. Comes, Chem. Phys. Letters 182 (1991) 290.
[69] K. Mikulecky, K.-H. Gericke and F.J. Comes. Ber. Bunsenges. Physik. Chem. 95 (1991) 927.
[70] P.A. Berg, J.J. Sloan and P.J. Kuntz, J. Chem. Phys. 95 (1991) 8038.
[71] R.J. Blint and M.D. Newton, Chem. Phys. Letters 32 (1975) 178.